

# Detection of Charge-Neutral Near-Equilibrium Processes at Na-Metal Electrodes by Electrochemical Microcalorimetry

Franziska Karcher, Matthias Uhl, Tanja Geng, Timo Jacob, and Rolf Schuster\*

Investigations on electrochemical kinetics usually rely on the measurement of current or potential as a function of time. Charge-neutral process steps or side reactions are naturally disguised in the electrical signals and have only indirect impact. However, all processes will contribute to heat evolution. In this work, heat absorption/liberation is measured as a function of time for pulsed Na deposition/dissolution on a Na-electrode in a 1 M NaPF<sub>6</sub>/diglyme solution, in addition to the standard electrochemical signals. While potential and current transients both exhibited sharp rectangular shapes, indicating instantaneous electrochemical Na deposition or dissolution on the time scale of the pulse (10 ms), heat absorption or liberation continued up to about 0.5 s after the pulse. Since heat evolution is to large extent reversible, this corresponded to entropy changes in the absence of external electric current flow, pointing to a reversible, charge-neutral chemical process accompanying Na deposition or dissolution. From the observed entropy changes, it is suggested that upon Na deposition solvated Na<sup>+</sup> ions are instantaneously transferred into the outer layers of the solid electrolyte interphase, followed by slow desolvation.

reduction is accompanied by desolvation of metal ions, ion transport through the solid electrolyte interphase (SEI), and possibly also by ongoing SEI formation processes.<sup>[1-3]</sup> In addition, also charge-neutral processes such as phase transformations, reordering of the interphase, or changes in the solvation state of ions near the electrode may occur. Since such charge-neutral processes do not contribute to the current, they are usually not directly detectable by electrochemical methods, although they might indirectly influence the charge transfer processes, for example, by changing the kinetics of the metal deposition processes. In situ methods such as X-ray diffraction or X-ray absorption spectroscopy are probably suitable to investigate such charge-neutral side processes, although their application might be hampered by limited time resolution and sensitivity.

## 1. Introduction

The charging of battery electrodes is usually a complicated multistep process. Even for simple alkali metal electrodes the

A promising alternative is to measure thermodynamic quantities such as the heat flux, which evolves at the electrode during a reaction.<sup>[4]</sup> Recently, we presented a study on sodium bulk metal deposition and dissolution from diglyme and propylene carbonate-based electrolytes.<sup>[5]</sup> We determined the heat, which was liberated or absorbed during the electrochemical reactions at a Na metal electrode with a specially designed microcalorimeter, where the temperature of a thin working electrode is measured at its backside with a pyroelectric sensor (see Refs. [4,6] and Supporting Information for the principle of the measurement). In that study, we focused on thermodynamic properties like the solvation entropy and the entropic contribution to the free enthalpy of the cell reaction and the half-cell potential, which were derived from the reversibly exchanged heat upon pulsed Na deposition or dissolution for 10 ms. While these quantities were obtained from the overall exchanged heat on a freshly prepared sodium surface, we observed that on aged Na electrodes considerable heat flux continued up to about 0.5 s after the current pulse, without external current flow, thus signaling charge-neutral processes following the electrochemically driven reduction or oxidation reaction.

In the current contribution, we will in detail discuss the time dependence of the heat flux at a Na metal electrode upon Na deposition or dissolution driven by short 10 ms potential pulses and disentangle the heat into the individual contributions from the different reaction steps of Na deposition/dissolution on an SEI-covered Na electrode. We will show that the heat flux is essentially reversible, that is, it changes its sign and retains its

F. Karcher, R. Schuster  
Institute of Physical Chemistry  
Karlsruhe Institute of Technology  
Karlsruhe Germany  
E-mail: rolf.schuster@kit.edu

M. Uhl, T. Geng, T. Jacob  
Institute of Electrochemistry  
Ulm University  
Ulm Germany

T. Jacob  
Helmholtz-Institute-Ulm (HIU) Electrochemical Energy Storage  
Ulm Germany

T. Jacob  
Karlsruhe Institute of Technology (KIT)  
Karlsruhe Germany

 The ORCID identification number(s) for the author(s) of this article can be found under <https://doi.org/10.1002/aenm.202302241>

© 2023 The Authors. Advanced Energy Materials published by Wiley-VCH GmbH. This is an open access article under the terms of the Creative Commons Attribution-NonCommercial-NoDerivs License, which permits use and distribution in any medium, provided the original work is properly cited, the use is non-commercial and no modifications or adaptations are made.

DOI: 10.1002/aenm.202302241

magnitude upon reversing the current direction, which points to near-equilibrium processes for all reaction steps. Albeit with freshly prepared Na electrodes, the “delayed” heat, generated without external current flow, amounted only to about 10% of the total heat, it increased to about 30% and more for properly aged electrodes. This signals considerable influence of the state of the electrode surface on the kinetics of the Na deposition or dissolution reaction. Finally, we will present a phenomenological model, which points to desolvation as a possible candidate for a charge-neutral process and which may explain heat evolution/absorption without electrochemical current flow.

## 2. Results and Discussion

### 2.1. Current, Potential, Temperature, and Heat Transients at a Na Metal Electrode

The single-electrode microcalorimetry experiments were conducted on ca. 3.7- $\mu\text{m}$  thick Na layers, which were electrochemically deposited onto a dendritic Cu current collector (see experimental section and Supporting Information). For all experiments presented here, we chose 1 M NaPF<sub>6</sub> in diglyme as electrolyte, since a stable SEI can be formed in this system (see Refs. [2,3,5,7–9] and references therein). The two upper panels of Figure 1a,b show potential and current transients upon 10 ms potential steps of  $\pm 100$  mV amplitude, causing Na deposition and dissolution on the Na layer, which in this case was completely dissolved and redeposited five times prior to the microcalorimetry experiment (in the following, this is called “aged” Na surface). The current and potential pulses nicely coincide and exhibit a rectangular shape, showing that Na deposition or dissolution proceed without relevant mass transport limitations or depletion of the electrolyte on the timescale of the 10 ms pulse. After the pulse, at  $t = 20$  ms, the cell was switched to open circuit conditions (OCP) and the potential immediately (within the 10  $\mu\text{s}$  time resolution of the data recording) jumped to  $<10$  mV deviation from the equilibrium potential and further relaxed to zero within the next 1 ms. It is noteworthy that the total charge, which flowed during the potential pulses, amounts to only 13  $\mu\text{C cm}^{-2}$ , which corresponds to deposition or dissolution of only 6% of a hypothetical Na monolayer.

The temperature changes as a function of time, measured at the backside of the electrode, are plotted in the third row of Figure 1a,b. Since in our home-built microcalorimeter, both, the electrode and the sensor are thin (total thickness of electrode-sensor assembly ca. 120  $\mu\text{m}$ ) and all materials are in intimate thermal contact, any temperature gradient across the electrode-sensor assembly, evolving from heat uptake at the electrode surface, will equilibrate rather quickly (within ca. 100  $\mu\text{s}$ , see Supporting Information).<sup>[6]</sup> Therefore, the sensor essentially monitors the electrode’s surface temperature during the experiment. Thus, the linear temperature fall (for deposition) or rise (for dissolution) in Figure 1 directly signal heat absorption or liberation, respectively, with approximately constant heat flux during the 10 ms electrochemical reaction at the electrode surface. This is in accordance with the current transients in the second-row panels of Figure 1, which show constant reaction current during the potential pulse. After the pulse, at  $t = 20$  ms, the electrochemical reactions cease and the temperature of the electrode

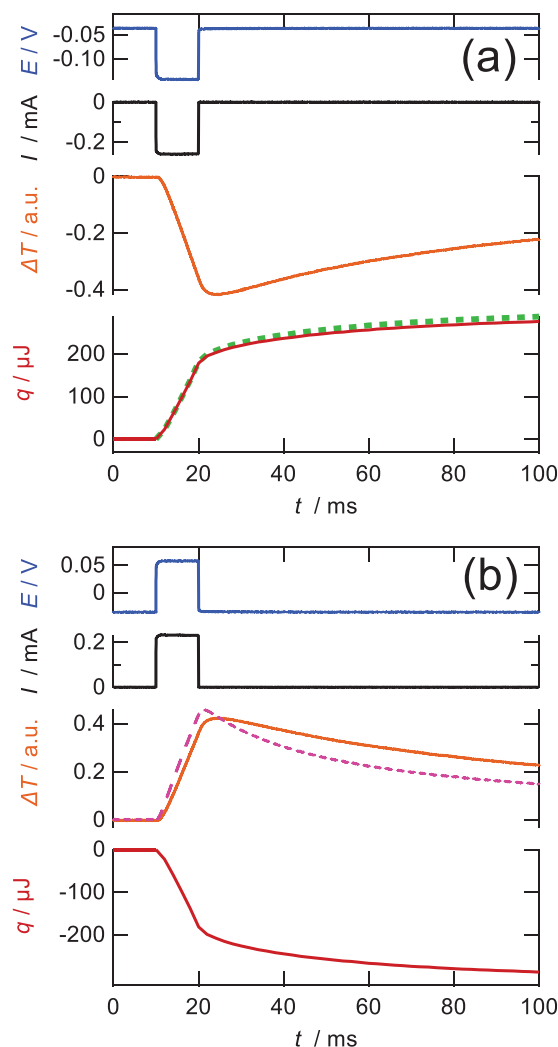


**Figure 1.** Potential (blue), current (black), temperature (orange), and heat (red) transients upon Na deposition a) and dissolution b) in 1 M NaPF<sub>6</sub> in diglyme with a 10 ms potential step, starting at  $t = 10$  ms at OCP. The experiments were conducted at an aged Na surface. After the potential pulse, at  $t = 20$  ms, the cell was again switched to OCP, thus suppressing any external current flow. The electrode temperature falls/rises about linearly during the potential pulse and relaxes toward its starting temperature after the pulse. The heat transients signal significant heat absorption a) or liberation b) also without external current flow. For comparison, we included the temperature transient following a 10 ms iron reduction in a [Fe(CN)<sub>6</sub>]<sup>3–4–</sup> solution, which clearly shows faster relaxation of the temperature than for Na deposition (pink dashed line in b)). To demonstrate reversibility of the Na deposition, we included the heat transient of b) with inverted sign in panel a) (green dotted line).

subsequently relaxes toward its starting temperature, due to heat dissipation into the surrounding cell and electrolyte. Heat dissipation into the electrolyte is expected to proceed much slower than temperature equilibration in the electrode-sensor assembly, due to the appreciably lower heat conductivity of the electrolyte, compared to that of the electrode-sensor assembly.<sup>[6]</sup> At first sight, heat dissipation seems to explain the temperature relaxation in Figure 1. However, for a more detailed comparison, we included the temperature variation for one of the fastest EC

reactions,<sup>[10]</sup> the reduction of  $[\text{Fe}(\text{CN})_6]^{3-}$  to  $[\text{Fe}(\text{CN})_6]^{4-}$  in aqueous electrolyte, as pink dashed line in the temperature panel of Figure 1b. With this reaction, the heat evolution stops immediately at the end of the current pulse. The depicted temperature transient was recorded in the same setup, directly following the Na experiments and was also used for calibration of the heat scale (see Ref. [5]). It can be clearly seen that the temperature relaxation following the electrochemical Fe reduction is considerably faster than that observed for Na deposition or dissolution. This strongly suggests that heat liberation or absorption is continuing in the case of Na deposition or dissolution also without external current flow. This becomes clearer by explicitly plotting the liberated or absorbed heat as a function of time, which can be obtained by deconvolution of the temperature signal with the thermal response function of the microcalorimeter (see Supporting Information and Refs. [6,11]). In the following, positive heat means transfer of heat from the surrounding to the electrode system in an ideal isothermal experiment. In an adiabatic experiment, heat is withdrawn from the electrode system, which would correspond to cooling. In the (quasi-adiabatic) single electrode microcalorimetry experiments, the temperature variation is typically in the range of  $\mu\text{K}$  to  $\text{mK}$  and hence, the experiment can be assumed to be conducted isothermally to a very good approximation. The resulting transients of the heat as a function of time are shown in the fourth rows of Figure 1. Obviously, about 30% of the heat at  $t = 100$  ms is generated or absorbed without any external current flow for the experiment in Figure 1, that is, after the end of the current pulse at  $t = 20$  ms. It should be noted that although in Figure 1 the data are plotted only up to  $t = 100$  ms, we generally determined the heat up to  $t = 0.5$  s. Indeed, for the experiments in Figure 1 heat evolution continued also after  $t = 100$  ms so that finally, at 0.5 s, ca. 50% of the heat was generated after the current pulse (see results below). The heat transients are highly reversible, which means that only their signs change upon reversing the current flow, whereas the overall shape and magnitude remain. To demonstrate this, we inverted the sign of the heat transient in Figure 1b and included it as dotted line in Figure 1a. The small difference may be ascribed to different conversions during the positive and the negative potential pulses as well as to a small contribution of irreversibly exchanged heat. The latter may be attributed to the overpotential of the charge transfer reaction, to concentration overpotential, due to emerging concentration gradients, or to Joule heat from ion migration in solution.<sup>[12]</sup>

## 2.2. Determination of the Reversible Heat $q_{\text{rev}}$ and Entropy Changes as a Function of Time

For further discussion, we will derive the time-dependent, reversibly exchanged heat from the experimental data. The reversibly exchanged heat,  $q_{\text{rev}}$ , determines the entropy change of the system, due to heat transfer from the surrounding,  $dS = \frac{\delta q_{\text{rev}}}{T}$ . In an isothermal half-cell system, it can be readily interpreted in terms of entropy changes due to (electro-) chemical processes inside the system. For example, this is in detail shown in a seminal review by Agar.<sup>[13]</sup> From rearrangement of equation 11 in Ref. [13] and adaption to the notation used here (see Supporting Information), it follows that the reaction entropy,  $\Delta_{\text{R}}S$ , of

the (electro-)chemical process is balanced by the entropy change from reversible heat transfer from surrounding,  $q_{\text{rev}}/T$ , plus the net entropy of transfer,  $\Delta_{\text{T}}S$ , due to the transport of heat by the migration of ions in the electrolyte and by electrons in the conductor across the border of the half cell<sup>[12,13]</sup>:

$$\Delta_{\text{R}}S = \Delta_{\text{T}}S + \frac{q_{\text{rev}}}{T} \quad (1)$$

Equation (1) is formulated with molar quantities, normalized to the electrochemical conversion, that is, the charge that flowed in the outer cell circuit during the potential pulse. Equation (1) can be readily transferred to time-dependent variables, with  $\Delta_{\text{R}}S(t)$  representing the entropy change up to time  $t$  by the (electro-)chemical reactions,  $\Delta_{\text{T}}S(t)$  stating the net entropy of transfer and  $q_{\text{rev}}(t)$  the reversibly exchanged heat at time  $t$ . In the limit of long times,  $\lim_{t \rightarrow \infty} \Delta_{\text{R}}S(t)$  then corresponds to the conventional reaction entropy of the overall (electro-)chemical reaction.

In order to determine the reversibly exchanged molar heat at time  $t$ ,  $q_{\text{rev}}(t)$ , we have to remove irreversible heat contributions due to overpotential and Joule heat from the heat transients. To accomplish this, we conducted typically more than 30 single microcalorimetry experiments for each investigated system, analogously to those in Figure 1, with varying potential pulse amplitudes and polarities and thus varying contributions from irreversibly exchanged heat. We normalized the heat measured at time  $t$  in a single microcalorimetry experiment by the charge, which flowed in the outer cell circuit during the 10 ms potential pulse. This normalized heat refers to the electrochemical conversion, that is, to moles of elementary charges, which flowed in the outer cell circuit during the potential pulse. Exemplarily two sets of the normalized heat values, at  $t = 20$  ms and  $t = 100$  ms, from 39 single microcalorimetry measurements on the aged Na surface used in Figure 1 are shown in Figure 2 as a function of the pulse amplitude. In accordance with the common sign convention, the normalized heat for the cathodic reaction, which corresponds to Na deposition, is plotted. Thus, positive normalized heat corresponds to cooling of the electrode upon negative potential pulses or heating upon positive ones. It can be seen from Figure 2, that with increasing absolute value of the pulse amplitude, the half cell becomes hotter per mole of charge for more positive pulses and less cold for more negative ones, signaling the evolution of heat due to irreversible processes. For the quantitative determination of the reversibly exchanged heat at times  $t = 20$  ms and  $t = 100$  ms, we interpolated the corresponding data in Figure 2 to zero overpotential, that is, zero pulse amplitude (dashed vertical line in Figure 2, filled symbols). One may argue that the reaction rates for forward and backward direction, that is, for different pulse polarities, might strongly differ and that therefore the extrapolation of the normalized heat at a given time  $t$  toward zero overpotential should be conducted independently for both pulse polarities. However, here we consider a near equilibrium process, where the system is relaxing to equilibrium after a short, relatively small perturbation (the total conversion for the data in Figure 2 is between 3% and 10% of a monolayer of Na on a hypothetically flat Na surface). For small enough perturbations, the relaxation into equilibrium proceeds exponentially with relaxation times that are a function of

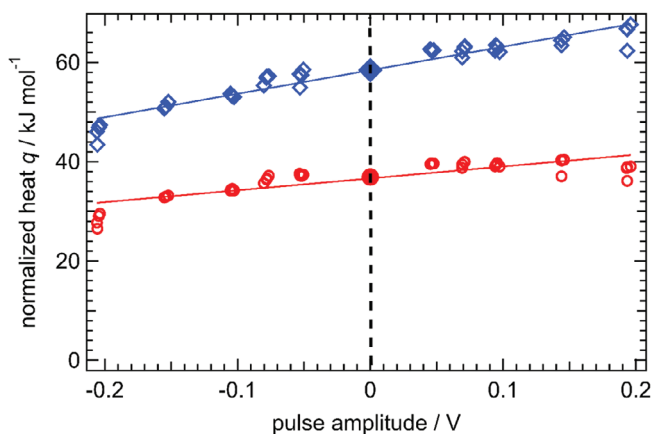


**Figure 2.** Normalized heat, that is, heat divided by moles of elementary charges, which flowed in the outer cell circuit during the potential pulse, extracted at  $t = 20$  ms (red open circles) and 100 ms (blue open diamonds) from the heat transients of potential pulse experiments on an aged Na surface with different pulse amplitudes and polarities. The interpolation toward zero overpotential (dashed vertical line) yields the reversibly exchanged molar heat at the electrode for  $t = 20$  ms and 100 ms (filled symbols). Positive sign means heat transfer from the surrounding to the electrode upon the cathodic electrode reaction in an isothermal experiment.

both, forward and backward reaction rates<sup>[14]</sup> and which are independent of the direction of the reaction. This justifies the simultaneous extrapolation of the normalized heat at a given time  $t$  toward zero overpotential for both positive and negative potential pulses. From the exemplary interpolation procedure for the datasets in Figure 2 we obtained  $q_{\text{rev}}(20 \text{ ms}) = 37 \text{ kJ mol}^{-1}$  and  $q_{\text{rev}}(100 \text{ ms}) = 58 \text{ kJ mol}^{-1}$ .

The above interpolation procedure was repeated for all times between the beginning of the electrochemical reaction up to 500 ms in time steps of 2 ms. The brown line in Figure 3 shows the result for the reversibly exchanged molar heat for Na deposition as a function of time for the aged Na surface of Figure 1. As stated in Equation (1),  $q_{\text{rev}}$  is directly correlated to the entropy change of the (electro-) chemical reaction. However, possible contributions originating from transport processes in the NaPF<sub>6</sub>/diglyme electrolyte have to be considered as well. These are in detail discussed in Ref. [5]. Since experimental values for the heat of transport of Na<sup>+</sup> and PF<sub>6</sub><sup>-</sup> in diglyme are not available, we employed the approximation suggested by Agar,<sup>[13]</sup> which yielded  $-5.3 \text{ kJ mol}^{-1}$  for the transport contribution to the heat from ion transport by migration, which is much smaller than the observed reversibly exchanged heat (up to ca.  $75 \text{ kJ mol}^{-1}$  in Figure 3). Furthermore, ion migration ceases after the potential pulse and the (small) concentration gradients of NaPF<sub>6</sub> in the electrolyte will equilibrate by diffusion, eventually canceling the heat of transport. Thus, neglecting contributions from the heat of transport will not change the overall picture and the reversibly exchanged heat corresponds to a good approximation to the time-dependent entropy change caused by the reaction:  $\Delta_{\text{R}}S(t) \approx q_{\text{rev}}(t)/T$ . In Figure 3,  $\Delta_{\text{R}}S(t)$  is included as right axis.

It is evident from Figure 3 that only about 50% of the total heat or entropy change at  $t = 0.5$  s evolved during the 10 ms current pulse for Na deposition on an aged Na surface. Since

the cell was switched to OCP at  $t = 20$  ms, the rest of the entropy change occurred without any external current flow, which indicates a reversible and charge-neutral process, that is, without net charge transfer across the electrolyte-solution boundary, following the electrochemical reaction step. To elucidate possibly involved reaction steps, similar data for a freshly prepared Na surface as well as for a Na surface deposited after cycling down to  $-0.3$  V versus Na/Na<sup>+</sup> prior to deposition of a thick Na film, are included in Figure 3 (for details on the surface preparation, see experimental section). On the freshly prepared Na surface (red), most of the reversibly exchanged heat or entropy change (ca. 90%) evolved up to the end of the current flow at  $t = 20$  ms (indicated by the vertical dashed line) and the heat flow effectively ceased at  $t = 100$  ms. In contrast, for the surface pretreated with negative potentials (green) the part of the heat, absorbed during the current pulse, amounts to only about 10%, while 90% being absorbed without external current flow.

Albeit the temporal distribution of the heat absorption strongly varies for different surface preparations, the total amount of heat at the end of the measurement at 0.5 s reaches about the same value of  $70\text{--}80 \text{ kJ mol}^{-1}$ . In Figure 3, we included error bars for  $t = 100$  ms and  $t = 0.5$  s, representing the standard deviation from 18 microcalorimetry measurement series on four different, freshly prepared Na surfaces. As expected, due to thermal drift, the error increases significantly for longer times. Considering the increasing baseline error for longer times, our data imply that for long times  $t \gtrsim 0.5$  s all heat transients will asymptotically reach about  $75 \text{ kJ mol}^{-1}$  corresponding to a net reaction entropy of about  $252 \text{ J mol}^{-1} \text{ K}^{-1}$  (ignoring transport contributions). This strongly supports that for all three surface preparations in Figure 3 the same net reversible reaction occurs, where solvated Na<sup>+</sup> ions are reduced and eventually deposited as bulk Na. Side processes such as SEI formation or reduction of water contaminations can be safely neglected since they presumably proceed irreversibly. Even if they proceeded reversibly, different total  $\Delta_{\text{R}}S$  values would be expected, depending on the surface state and rate of side reactions.

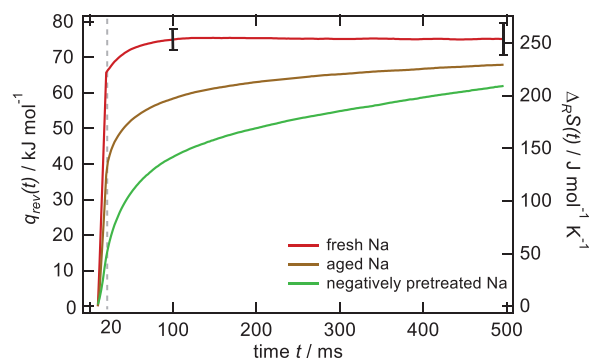


**Figure 3.** Reversibly exchanged molar heat as a function of time upon Na deposition or dissolution with 10 ms potential pulses for three different surface preparations, a fresh Na film (red), an aged Na film (brown), and a Na film on a negatively pretreated electrode surface (green). The pretreatment has strong influence on the amount of heat absorption/liberation after the current flow ( $t > 20$  ms).

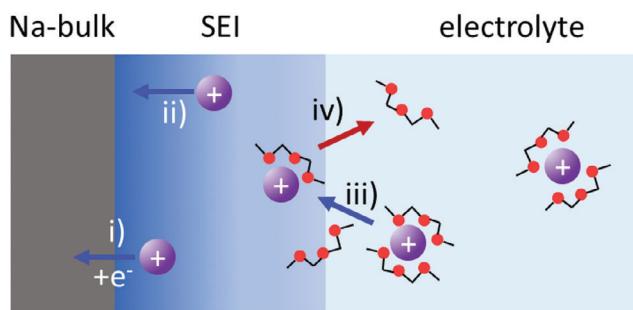


**Figure 4.** Phenomenological model of the sub processes of the electrochemical Na deposition on an SEI covered electrode. (Partly) solvated  $\text{Na}^+$  is transferred from the bulk of the electrolyte solution in the SEI (iii), where it is transported by ion migration (ii) and eventually reduced (i). From our measurements we conclude that these electrochemical steps proceed fast, within the 10 ms potential pulse. In parallel slow chemical desolvation of the  $\text{Na}^+$  ions takes place (iv).

### 2.3. Implications for the Reaction Steps of Na Deposition and Dissolution

Summarizing the results so far, we observed that Na metal deposition proceeds via at least two partly overlapping reversible processes, an electrochemical process, where charge is transported across the electrode-electrolyte boundary, and a slower close-to-equilibrium process, where heat is liberated or absorbed without external current flow and whose kinetics is strongly influenced by the surface preparation of the Na-surface. The net reaction entropy,  $\Delta_{\text{R}}S$ , is positive and independent of the surface preparation. Furthermore, the quasi-instantaneous potential relaxation toward the equilibrium potential after the potential step (see Figure 1), which was observed for all three surface preparations, signals that the charge carriers reached their equilibrium distribution in the interface immediately after the end of the current pulse. Note that at equilibrium the potential drop across the ionically conducting SEI will be zero, since otherwise the  $\text{Na}^+$  ions would redistribute in the SEI and the potential relaxation would continue. For the equilibrium charge distribution the potential will thus solely drop at the metal/SEI and SEI/electrolyte interfaces, where double-layer-like charge distributions will evolve.

How can such sub-processes be conceived within the framework of an overall Na deposition process? As sketched in **Figure 4**, slightly extending the mechanism suggested in Refs. [9,15], Na deposition on a Na surface may be formally divided into four phenomenological steps: i) the basic electrochemical reduction of  $\text{Na}^+$  to Na at the interface between the SEI layer and the Na surface by electrons from the electrode, ii) the transport of  $\text{Na}^+$  ions in the SEI, and iii) the transfer of  $\text{Na}^+$  ions from the solution into the SEI. These steps are accompanied by iv) the desolvation of the  $\text{Na}^+$  ions. The first three steps are of electrochemical nature, involving charge transfer across a phase or phase boundary. The desolvation step is purely chemical and does not involve transfer of charge. A priori it is not clear, where and when desolvation occurs. In one extreme, it will happen in parallel with process iii), the incorporation of the  $\text{Na}^+$  from solution into the outer SEI layer. In the other extreme, solvated  $\text{Na}^+$  may be incorporated into the SEI and the ions will desolvate only upon reduction of  $\text{Na}^+$  at the metal surface.

The origin of the entropy changes during Na metal deposition in  $\text{NaPF}_6$ /diglyme was discussed in detail in Ref. [5]. There it was found that the overall entropy change of  $234 \text{ J mol}^{-1} \text{ K}^{-1}$ <sup>[16]</sup> is dominated by desolvation of  $\text{Na}^+$ , that is, by liberation of solvent molecules in the first solvation shell ( $191 \text{ J mol}^{-1} \text{ K}^{-1}$ ) and release of Born entropy from higher solvation shells ( $81 \text{ J mol}^{-1} \text{ K}^{-1}$ ), which strongly overcompensate the entropy loss by fixation of Na at the electrode ( $-37,5 \text{ J mol}^{-1} \text{ K}^{-1}$ ). Thus, most of the entropy changes upon Na deposition can be attributed to the desolvation step (formal step iv) from above), while the electrochemical reaction steps (formal steps i) to iii)) will affect only the entropy change upon the fixation of Na. In other words, the temporal behavior of the entropy change  $\Delta_{\text{R}}S(t)$  in Figure 3 predominantly signals the progress of desolvation step iv). In conclusion, for the aged or negatively pre-polarized Na surface in Figure 3 (brown and green lines), where most of the heat was absorbed after the potential pulse, the desolvation process proceeded to a large extent after the electrochemical current flow. In addition, it is unlikely that  $\text{Na}^+$  reduction at the SEI/electrode interface (process i)) or transfer of  $\text{Na}^+$  from solution into the SEI (process iii)) significantly continued after the current pulse, since in the absence of external current flow this would lead to discharging of the corresponding interface capacitances and thus to significant changes of the electrode potential.<sup>[6]</sup> Therefore, the electrochemical steps proceeded fast, that is, within the 10 ms current flow, without significant charging of the interface capacitance. As a consequence, the amount of  $\text{Na}^+$  ions reduced at the SEI-electrode boundary has to match the amount of  $\text{Na}^+$  ions entering the SEI from the solution side during the 10 ms current flow.

This apparent contradiction between fast  $\text{Na}^+$  transfer from solution to the SEI and slow desolvation can be resolved, assuming the transfer of (at least partly) solvated  $\text{Na}^+$  from the solution into the SEI during the potential pulse. This way, charging of the SEI during the potential pulse is avoided and desolvation entropy is not produced yet. Such a transfer of (partially) solvated  $\text{Na}^+$  into the SEI also naturally explains the dependence of  $\Delta_{\text{R}}S(t)$  on the pretreatment of the surface. The pretreatment influences the structure and porosity of the SEI and therefore the degree to which the solvation shell may be transferred to the SEI.<sup>[1,15]</sup> It is also reasonable to expect that the temporal behavior of the heat evolution will depend on the employed solvent and electrolyte, since the degree of solvent incorporation into the SEI will strongly depend on the cell chemistry, because of both, the varying composition and structure of the SEI as well as the nature of the incorporated solvent molecules. Jensen et al. studied the solvation of  $\text{Na}^+$  in diglyme by neutron diffraction.<sup>[17]</sup> They found that the solvation structure of the prevalent  $\text{Na}^+(\text{diglyme})_2$  complex may promote the observed cointercalation of  $\text{Na}^+$  and solvent into graphite. Perhaps similar mechanisms may be operative also for the proposed transfer of solvated  $\text{Na}^+$  into the SEI in the presence of diglyme. Indeed, we performed similar experiments on Na deposition in 1 M  $\text{NaClO}_4$  in propylene carbonate (PC) (see Figure S1, Supporting Information). In this electrolyte about 90% of the heat evolution occurred during the 10 ms potential pulse, irrespective of the pretreatment of the Na-electrode surface, implying much less involvement of PC solvent molecules in the charge-neutral processes continuing after the electrochemical reaction steps.

From our experiments, we cannot draw strong conclusions on where the desolvation process takes place. Note however, that under our experimental conditions (short potential pulses, minute conversion) desolvation is a reversible process. One may speculate that reversible exchange of solvent molecules is more easily established in the outer SEI, where the SEI may be rougher or more porous and where the diffusion length is short. For the SEI in Li-ion batteries such a heterogeneous nature of the SEI film structure, where a less dense, porous organic layer is covering a dense inorganic SEI, is well-accepted (Refs. [1,15] and references therein). Also for NaPF<sub>6</sub> in diglyme the formation of a thin, organic-rich layer on top of a compact inorganic SEI largely consisting of Na<sub>2</sub>O and NaF was found.<sup>[7]</sup> Lim et al. reported a particularly porous SEI for NaCF<sub>3</sub>SO<sub>3</sub>/triglyme electrolytes, whereas in carbonate-based electrolytes a denser SEI was formed.<sup>[18]</sup> The latter observation is in line with our finding that heat evolution becomes most delayed in diglyme solutions, while in PC solutions heat evolution stopped at about 100 ms. The other extreme, that the solvation shell is retained up to the electrode/SEI boundary, seems rather unlikely, since in that case desolvation had to proceed in parallel to reduction of Na<sup>+</sup>, which contradicts the considerable heat evolution after the potential pulse. Furthermore, penetration of solvent up to the metal surface would spoil the electronically insulating effect of the SEI, which is thought to prevent electrolyte reduction. The above-described phenomenological model provides a rather simplified view on the Na deposition process and more sophisticated, generic models, including, for example, adsorption of Na<sup>+</sup> ions and double layer charging at the SEI/solution interface may be needed for a more realistic description of the interface processes.<sup>[19]</sup> However, the general observation of our experiments, that there is a continuing chemical process extending well beyond the purely electrochemical processes, prevails irrespective of its mechanistic interpretation.

### 3. Conclusion

Time-dependent detection of the heat evolution or absorption during the electrochemical Na deposition in NaPF<sub>6</sub>/diglyme revealed that its detailed kinetics is strongly determined by the actual condition of the surface. Albeit the electrochemical current flow suggested the almost instantaneous Na deposition on a ms time scale, the continuing heat absorption indicates slow process steps of chemical nature, which are not directly detectable by purely electrochemical measurements. By combining results from both, pulsed electrochemical measurements and time-dependent heat measurements, we propose fast electrochemical Na<sup>+</sup> reduction accompanied by almost instantaneous refilling of the SEI by Na<sup>+</sup> ions from solution. However, the accompanying desolvation of the Na<sup>+</sup> is a slow process, suggesting that solvated Na<sup>+</sup> ions are incorporated in the SEI during the electrochemical current flow such that desolvation is continuing inside the SEI. Under our process conditions, that is, with minute electrochemical conversions, the overall deviations from thermodynamic equilibrium during the chemical desolvation process remained small, so that the latter process did not lead to significant overpotentials during Na<sup>+</sup> deposition, even on aged or negatively pretreated Na surfaces. However, this might change upon continuous charging or discharging conditions where such slow chemical desolvation processes, which are usually disguised

in electrochemical measurements, might hinder the transport of Na<sup>+</sup> in the SEI. Thus, the transport of Na<sup>+</sup> across the SEI may become rate limiting, in line with findings for Li and Na ion batteries.<sup>[1,9,20]</sup>

### 4. Experimental Section

Temperature changes at a single Na electrode have been determined in our home-built microcalorimeter<sup>[6,11]</sup> (see Supporting information for further details), where we measured the temperature at the backside of a thin, Na-plated Cu current collector with a thin pyroelectric sensor (overall thickness of the electrode-sensor assembly ca. 120 μm). At the Na-covered front side of the electrode, the electrochemical cell body has been mounted. For the preparation of the reference and counter electrodes (Na wires) and the electrolyte solutions as well as further experimental details see Supporting Information and Refs. [5,21] and references therein. Due to the intimate thermal contact between the sensor and the electrode and the low heat capacity of the thin sensor electrode assembly, temperature changes at the electrode surface have been instantaneously measured at the time scale of the experiment, that is, up to about 1 s with a time resolution of about 1 ms.

The Cu current collector was in situ plated with a ca. 3.7 μm thick Na-layer prior to our calorimetry experiments to provide a well-defined Na metal electrode as working electrode. The thickness has been estimated from the deposition charge, assuming a homogeneous Na layer. For the reproducible preparation of a fresh Na layer with minimum retarded heat liberation/absorption, we established a procedure, which is described in detail in Ref. [5] and which essentially consists of 10 times cycling between 3 V and 0 V versus Na/Na<sup>+</sup> followed by electrochemical plating of Na with a current density of −1.25 mA cm<sup>−2</sup> for about 20 min. In microcalorimetry experiments on this surface about 90% of the heat evolved during the 10 ms potential pulse. Heat evolution essentially stopped at  $t \approx 100$  ms as shown in Figure 3 (red line). Defined aging of this surface has been achieved by dissolving and redepositing the Na layer five times, analogously to the preparation of the fresh Na surface. Surfaces obtained by this procedure reproducibly showed the behavior, tagged “aged surface” in Figures 1 and 3, where about 50% of the heat flowed after the 10 ms potential pulse. Negative pretreatment of the surface by cycling the Cu current collector ten times between −0.3 V and 3 V, before depositing a thick Na layer by the procedure described above for the fresh Na surface, yielded even stronger retardation of the heat evolution (denoted as “negatively pretreated” in Figure 3).

### Supporting Information

Supporting Information is available from the Wiley Online Library or from the author.

### Acknowledgements

The authors would like to thank Julian Becherer, Stefan Mück, Reiner Mönig, Krishnaveni Palanisamy, and Christine Kranz for providing the electrolyte solutions. Discussions with Arnulf Latz are gratefully acknowledged. This work contributes to the research performed at CELEST (Center for Electrochemical Energy Storage Ulm-Karlsruhe) and was funded by the Deutsche Forschungsgemeinschaft (German Research Foundation, DFG) under Germany's Excellence Strategy EXC 2154, Project ID 390874152 (POLIS Cluster of Excellence).

Open access funding enabled and organized by Projekt DEAL.

### Conflict of Interest

The authors declare no conflicts of interest.

## Data Availability Statement

The data that support the findings of this study are openly available in zenodo at <https://zenodo.org/records/10039787>, reference number 10039787.

## Keywords

desolvation kinetics, electrochemical microcalorimetry, sodium metal deposition, solid electrolyte interphase

Received: July 13, 2023

Revised: October 18, 2023

Published online:

- 
- [1] S. Shi, P. Lu, Z. Liu, Y. Qi, L. G. Hector, H. Li, S. J. Harris, *J. Am. Chem. Soc.* **2012**, *134*, 15476.
- [2] Y. Li, F. Wu, Y. Li, M. Liu, X. Feng, Y. Bai, C. Wu, *Chem. Soc. Rev.* **2022**, *51*, 4484.
- [3] S. K. Vineeth, C. B. Soni, Y. Sun, V. Kumar, Z. W. Seh, *Trends Chem.* **2022**, *4*, 48.
- [4] R. Schuster, *Curr. Opin. Electrochem.* **2017**, *1*, 88.
- [5] F. Karcher, M. Uhl, T. Geng, T. Jacob, R. Schuster, *Angew. Chem., Int. Ed.* **2023**, *62*, e202301253.
- [6] K. R. Bickel, K. D. Etzel, V. Halka, R. Schuster, *Electrochim. Acta* **2013**, *112*, 801.
- [7] Z. W. Seh, J. Sun, Y. Sun, Y. Cui, *ACS Cent. Sci.* **2015**, *1*, 449.
- [8] K. Westman, R. Dugas, P. Jankowski, W. Wieczorek, G. Gachot, M. Morcrette, E. Irisarri, A. Ponrouch, M. R. Palacín, J.-M. Tarascon, P. Johansson, *ACS Appl. Energy Mater.* **2018**, *1*, 2671.
- [9] J. Song, B. Xiao, Y. Lin, K. Xu, X. Li, *Adv. Energy Mater.* **2018**, *8*, 1703082.
- [10] a) L. M. Peter, W. Dürr, P. Bindra, H. Gerischer, *J. Electroanal. Chem. Interfacial Electrochem.* **1976**, *71*, 31; b) M. Schönig, R. Schuster, *Appl. Phys. Lett.* **2020**, *116*, 91601.
- [11] S. Frittmann, V. Halka, C. Jaramillo, R. Schuster, *Rev. Sci. Instrum.* **2015**, *86*, 64102.
- [12] T. Ozeki, N. Ogawa, K. Aikawa, I. Watanabe, S. Ikeda, *J. Electroanal. Chem. Interfacial Electrochem.* **1983**, *145*, 53.
- [13] J. N. Agar, in *Advances in Electrochemistry And Electrochemical Engineering* (Ed: P. Delehay), Interscience Publisher, London **1963**, pp. 31–121.
- [14] J. I. Steinfeld, J. S. Francisco, W. L. Hase, *Chemical kinetics and dynamics*, Prentice Hall, Upper Saddle River, NJ, **1999**.
- [15] E. Peled, S. Menkin, *J. Electrochem. Soc.* **2017**, *164*, A1703.
- [16] The entropy deviates slightly from the number given in the current work, since it contains the correction for the entropy of transfer.
- [17] A. C. S. Jensen, H. Au, S. Gärtner, M.-M. Titirici, A. J. Drew, *Batteries Supercaps* **2020**, *3*, 1306.
- [18] K. Lim, B. Fenk, J. Popovic, J. Maier, *ACS Appl. Mater. Interfaces* **2021**, *13*, 51767.
- [19] a) J. Lück, A. Latz, *Phys. Chem. Chem. Phys.* **2016**, *18*, 17799; b) J. Lück, A. Latz, *Phys. Chem. Chem. Phys.* **2018**, *20*, 27804.
- [20] H. Yildirim, A. Kinaci, M. K. Y. Chan, J. P. Greeley, *ACS Appl. Mater. Interfaces* **2015**, *7*, 18985.
- [21] M. Schönig, S. Frittmann, R. Schuster, *ChemPhysChem* **2022**, *23*, 202200227.